Published in final edited form as:
Dev Cell. 2009 August ; 17(2): 257–267. doi:10.1016/j.devcel.2009.06.012.

Phospho-regulated interaction between kinesin-6 klp9p and microtubule bundler ase1p promotes spindle elongation

Chuanhai Fu[1], **Jonathan J. Ward**[2], **Isabelle Loiodice**[1,3], **Guilhem Velve-Casquillas**[1,3], **Francois J. Nedelec**[2,*], and **Phong T. Tran**[1,3,*]

[1] Cell and Developmental Biology, University of Pennsylvania, Philadelphia, PA 10104, USA

[2] Cell Biology and Biophysics Program, EMBL, Heidelberg 69117, GERMANY

[3] Institut Curie – CNRS UMR144, Paris 75005, FRANCE

Abstract

The spindle midzone – composed of antiparallel microtubules, microtubule-associated proteins (MAPs), and motors – is the structure responsible for microtubule organization and sliding during anaphase B. In general, MAPs and motors stabilize the midzone and motors produce sliding. We show that fission yeast kinesin-6 motor klp9p binds to the microtubule antiparallel bundler ase1p at the midzone at anaphase B onset. This interaction depends upon the phosphorylation states of klp9p and ase1p. The cyclin-dependent kinase cdc2p phosphorylates and its antagonist phosphatase clp1p dephosphorylates klp9p and ase1p to control the position and timing of klp9p-ase1p interaction. Failure of klp9p-ase1p binding leads to decreased spindle elongation velocity. The ase1p-mediated recruitment of klp9p to the midzone accelerates pole separation, as suggested by computer simulation. Our findings indicate that a phosphorylation switch controls the spatial-temporal interactions of motors and MAPs for proper anaphase B, and suggest a mechanism whereby a specific motor-MAP conformation enables efficient microtubule sliding.

Introduction

Mitosis occurs in distinct phases defined by changes in chromosome and spindle dynamics. In general, bipolar spindle formation occurs in prophase. Chromosome capture and alignment occur in metaphase. Chromosome segregation occurs in anaphase. Telophase marks spindle breakdown and the start of cytokinesis. Anaphase is further categorized as anaphase A, where the chromosomes are segregated to the spindle poles; and anaphase B, where the spindle can undergo dramatic elongation to ensure that the segregated chromosomes are further separated. While mechanisms of chromosome segregation during anaphase A have been the focus of intense studies (Cheeseman and Desai, 2008; Tanaka and Desai, 2008), mechanisms regulating spindle elongation during anaphase B are less well understood, and may require complex interplay between regulatory proteins, motors and MAPs.

Anaphase B requires a proper bipolar spindle containing the midzone, a region of interdigitating microtubule overlap half-way between the spindle poles. In eukaryotes, the

*Correspondance: tranp@mail.med.upenn.edu and nedelec@embl.de.

conserved microtubule-associated protein Ase1/PRC1, the mitotic kinesin-5 motor and dynein play important roles in the formation of the spindle midzone and subsequent force production for spindle elongation (Maiato et al., 2004; Mogilner et al., 2006; Scholey et al., 2003; Sharp et al., 2000). Ase1/PRC1 bundles antiparallel microtubules at the midzone and gives structural integrity to the spindle. Cells lacking functional Ase1/PRC1 exhibit disorganized midzone microtubules and subsequent collapsed or broken spindles during metaphase and anaphase (Loiodice et al., 2005; Mollinari et al., 2002; Schuyler et al., 2003; Verni et al., 2004; Yamashita et al., 2005). Kinesin-5 (e.g., human Eg5) localizes at the poles and the midzone. Cells lacking functional kinesin-5 form mono-polar spindles early in mitosis (Hagan and Yanagida, 1990; Hagan and Yanagida, 1992; Hoyt et al., 1992; Kapoor et al., 2000; Roof et al., 1992). During anaphase B, kinesin-5 can produce force to slide midzone microtubules outward, thus producing spindle elongation (Kapitein et al., 2005; Straight et al., 1998). Interestingly, dynein plays a role during anaphase B without the need to localize at the spindle midzone. Dynein localizes to the cell cortex and interacts with the spindle pole-nucleated astral microtubules to produce pulling forces, which lengthens the spindle during anaphase B (Carminati and Stearns, 1997; Fink et al., 2006; Nguyen-Ngoc et al., 2007; O'Connell and Wang, 2000; Schmidt et al., 2005).

Other mitotic motors located at the spindle midzone include kinesin-4 (e.g., human KIF14) and kinesin-6 (e.g., human CHO1 and MKLP1). Surprisingly, they have not been implicated in spindle elongation during anaphase B. Instead, they appear to play a signaling role at telophase to regulate subsequent cytokinesis. Cells lacking functional kinesin-4 or kinesin-6 failed to complete cytokinesis (Gruneberg et al., 2006; Kuriyama et al., 2002; Matuliene and Kuriyama, 2002; Mishima et al., 2002).

Motors and MAPs act in concert throughout mitosis. Their interactions are often regulated by kinases and phosphatases in a cell cycle-dependent manner. It appears that Ase1/PRC1 is phosphorylated by the cyclin-dependent kinase Cdk1, and dephosphorylated Cdk1-antagonist phosphatase Cdc14. Phospho-regulation allows Ase1/PRC1 to act as a major scaffolding protein at the midzone to recruit motors, MAPs, and other regulatory proteins (Gruneberg et al., 2006; Jiang et al., 1998; Khmelinskii et al., 2007; Kurasawa et al., 2004; Zhu and Jiang, 2005; Zhu et al., 2006). Current reports on phospho-regulation of Ase1/PRC1 at the spindle midzone dealt primarily with its subsequent role as a scaffold for other proteins involved in cytokinesis, and not with its role in spindle elongation (Jiang et al., 1998; Khmelinskii et al., 2007; Zhu and Jiang, 2005).

The fission yeast *Schizosaccaromyces pombe* is a good model to study mechanisms of anaphase B. It has distinct phases of mitosis which resemble mammalian cells, and in particular, a prominent anaphase B characterized by dramatic spindle elongation (Mallavarapu et al., 1999; Nabeshima et al., 1998; Sagolla et al., 2003). Importantly, fission yeast lacks dynein-dependent astral microtubule pulling forces and kinesin-dependent microtubule flux at the spindle poles that are present in higher eukaryotes (Khodjakov et al., 2004; Tolic-Norrelykke et al., 2004), making its spindle midzone the sole structure responsible for anaphase B, and thus relatively simple for molecular dissection.

We describe here a novel function of the fission yeast kinesin-6 klp9p. Using a combination of biochemistry and live cell imaging analyses we show that prior to anaphase B, cdc2p (homolog of Cdk1) phosphorylates klp9p and the microtubule bundler ase1p, which maintains their spatial separation. At the onset of anaphase B, clp1p (also known as flp1p (Cueille et al., 2001), homolog of Cdc14) dephosphorylates klp9p and ase1p, allowing them to physically bind to each other at the spindle midzone to initiate spindle elongation. Deletion of klp9p and/or the motor-dead version of klp9p attenuate spindle elongation velocity. Phosphomimic versions of klp9p and ase1p and/or the inactive version of the

phosphatase clp1p also attenuate spindle elongation velocity. FRAP analyses show that klp9p and ase1p are more mobile when not interacting with each other. Using computer simulation we predict that optimal spindle elongation may only be achieved when flexible klp9p binds to and adopts the antiparallel configuration of ase1p. Our results define a molecular pathway linking motors and MAPs, and cell cycle-dependent regulatory kinases and phosphatases.

Results

Fission yeast has distinct phases during mitosis (Fig. 1A) (Mallavarapu et al., 1999;Nabeshima et al., 1998;Sagolla et al., 2003). In particular, anaphase B shows a well-defined increase in spindle length and spindle elongation velocity (Fig. 1B). We reasoned that anaphase B is likely to require molecular motors located along the spindle midzone to produce sliding forces. We therefore examined the localization of motors to the midzone by imaging GFP-tagged versions, and tested all motors for defects in spindle elongation by imaging individual motor deletion or mutant.

The fission yeast genome has 9 kinesins (*pkl1*$^+$, *klp2*$^+$, *klp3*$^+$, *tea2*$^+$, *klp5*$^+$, *klp6*$^+$, *cut7*$^+$, *klp8*$^+$, and an uncharacterized SPBC2D10.21c) and 1 dynein (*dhc1*$^+$). Sequence analysis revealed that the uncharacterized kinesin belongs to the kinesin-6 family. We named it *klp9*$^+$. Deletion of *klp9*$^+$ produced viable cells (see below). Individual deletion of all other motors have been reported to also produce viable cells, except for *cut7*$^+$ (Brazer et al., 2000; Browning et al., 2000; Garcia et al., 2002a; Garcia et al., 2002b; Hagan and Yanagida, 1990; Hagan and Yanagida, 1992; Hiraoka et al., 2000; Pidoux et al., 1996; Troxell et al., 2001; West et al., 2002; West et al., 2001). We therefore compared anaphase B velocities of wildtype and all motor deletion strains. Strains *dhc1Δ*, *pklΔ*, *klp2Δ*, *klp3Δ*, *tea2Δ*, *klp5Δ*, and *klp6Δ* all showed similar spindle elongation velocities during anaphase B compared to wildtype (Fig. 1E). (Parameters of spindle dynamics throughout this study are summarized in supplemental Table S3, S4, and S5).

Deletion of kinesin-5 *cut7*$^+$ was not viable, so we tested the nonfunctional temperature-sensitive mutant *cut7-24* (Hagan and Yanagida, 1990; Hagan and Yanagida, 1992). We constructed a microfluidic temperature-control device (to be published elsewhere), which allows rapid (10-sec) and robust temperature shift between 23°C – 35°C, while cells are being imaged on the microscope. *Cut7-24* cells were first imaged at the permissive 23°C, where cells were in various stages of the cell cycle. We then shifted and maintained cells at the non-permissive 35°C. Interphase cells subsequently became blocked in mitosis, exhibiting mono-polar spindles consistent with previous reports (Hagan and Yanagida, 1990; Hagan and Yanagida, 1992). In some instances, we were able to observe two adjacent cells going through mitosis (Fig. 1C). The metaphase cell, when shifted to 35°C, exhibited spindle collapse and became a mono-polar spindle within 2 minutes after temperature shift (Fig. 1C). The mono-polar spindle was a terminal phenotype. This suggested that the *cut7-24* mutant responds within 2 minutes of temperature shift, and is a relatively fast-acting mutant. Interestingly, the adjacent anaphase cell continued through anaphase B (Fig. 1C), at similar anaphase B velocity as wildtype cells at the same 35°C temperature (Fig. 1E). This indicated that *cut7*$^+$ is important for spindle formation and structural integrity of the metaphase spindle (Hagan and Yanagida, 1990; Hagan and Yanagida, 1992), but may not be important for anaphase B spindle elongation. Consistent with its lack of effect on anaphase B velocity, we failed to observe cut7p-3GFP at the spindle midzone during anaphase B (Fig. 1D).

Our analyses of all motors revealed that only *klp9Δ* showed significant decrease in anaphase B velocity at both temperature ranges (Fig. 1E). We note that there may be other

unidentified mechanisms responsible for microtubule-sliding during anaphase B which contributes to the total anaphase B velocity, such as different motors acting in concert. Nevertheless, *klp9*$^{+}$ alone suffices to account for the majority of anaphase B velocity. We next focused on the function of *klp9*$^{+}$.

Klp9p is a kinesin-6 involved in anaphase B spindle elongation

First, we examined the dynamics of klp9p throughout the cell cycle in conjunction with microtubules. From interphase to the onset of anaphase B, klp9p-GFP localized isotropically in the nucleoplasm (Fig 2A). At the onset of anaphase B, klp9p bound dramatically to the spindle and appeared to focus at the spindle midzone, the site of antiparallel overlapping microtubules (Fig. 2A). At the end of anaphase B, klp9p localized briefly to the so-called post-anaphase arrays (PAA) of microtubules (Hagan, 1998), before returning to the nucleoplasm (Fig. 2A). Klp9p localization to the spindle midzone and PAA microtubules appeared consistent with previously reported roles for the kinesin-6 family in regulating the exit from mitosis and the entry into cytokinesis (Guse et al., 2005;Kuriyama et al., 2002;Matuliene and Kuriyama, 2002;Mishima et al., 2004). However, kymograph showing that klp9p localization at the spindle midzone coincides with the onset of anaphase B (Fig 2B), and the result that *klp9Δ* cells showed decreased anaphase B spindle elongation velocity (Fig. 1E), prompted us to investigate its role in spindle elongation.

In vitro binding assays of recombinant klp9p revealed that it can exist in dimeric and tetrameric forms (Fig. 2C), thus implying that it can cross-link and slide microtubules apart, similar to the kinesin-5 Eg5 (Kapitein et al., 2005). Therefore, we examined the deletion and the motor-dead (md) version of klp9p. The motor-dead *klp9*^{md} has a mutated ATP-hydrolysis domain rendering the motor head inactive (Matuliene and Kuriyama, 2002). Wildtype, *klp9Δ*, *klp9Δ* cells expressing *klp9*^{md}, and *klp9Δ* cells expressing *klp9*^{wt} were assayed for anaphase B spindle elongation (Fig. 2D). Wildtype and *klp9Δ* cells expressing *klp9*^{wt} exhibited similar anaphase B velocities (mean ± sd: 0.67 ± 0.06 n=13 and 0.58 ± 0.04 n=11 μm/min, respectively), indicating that *klp9*^{wt} can rescue the *klp9Δ* deletion phenotype. In contrast, *klp9Δ* cells and *klp9Δ* cells expressing *klp9*^{md} showed significantly decreased velocities (0.30 ± 0.06 n=11 and 0.30 ± 0.04 n=10 μm/min, respectively). We hypothesize that the novel fission yeast klp9p is a kinesin-6 involved in generating microtubule-sliding forces at the spindle midzone during anaphase B. This may be a novel function for the kinesin-6 family.

Klp9p interacts physically with ase1p at the spindle midzone

We and others have previously reported that fission yeast ase1p localizes to the spindle midzone and functions to stabilize the bipolar spindle (Fig. 1A) (Loiodice et al., 2005;Yamashita et al., 2005), and that ase1p can autonomously target antiparallel microtubule overlap regions *in vitro* (Janson et al., 2007). In contrast, PRC1 has been reported to directly bind to the kinesin-4 KIF4 in order to be targeted to the spindle midzone in mammalian cells (Kurasawa et al., 2004;Zhu and Jiang, 2005). As there appears to be no homologues of kinesin-4 in fission yeast, we examined the interdependency of klp9p and ase1p targeting to the spindle midzone. Imaging revealed that at the onset of anaphase B ase1p always appeared at the spindle midzone a few seconds before klp9p (Fig. 3A). This suggests that ase1p binds to the spindle midzone earlier and independently of klp9p. We then hypothesized that ase1p may recruit klp9p to the spindle midzone.

To test this hypothesis, we examined klp9p distribution in the absence of *ase1*$^{+}$. Whereas wildtype cells showed distinct and focused klp9p at the spindle midzone during anaphase B, *ase1Δ* cells showed dispersed klp9p localization throughout the spindle (Fig. 3B), consistent with ase1p recruiting klp9p to the spindle midzone. Interestingly, ase1p also showed

dispersed localization in *klp9Δ* cells (Fig. 3C), suggesting that once bound together, klp9p can transport and focus ase1p to the spindle midzone (Zhu et al., 2005;Zhu and Jiang, 2005). To further test for physical interactions between klp9p and ase1p, we performed *in vitro* binding assays of recombinant klp9p and ase1p. Klp9p was observed to bind directly to ase1p (Fig. 3D). Our mapping studies reveal that the domain responsible for binding klp9p lies at $ase1^{416–639}$ (Fig. 3D). Taken together, we hypothesize that klp9p can bind autonomously to the spindle microtubules at the onset of anaphase B, but efficient targeting to the midzone requires physical binding to ase1p. Importantly, the *klp9Δ-ase1Δ* double-deletion are synthetically lethal (our unpublished data), suggesting that this combination of motor and MAP is essential for anaphase B spindle elongation.

Cdc2p and clp1p regulates the phosphorylation states of klp9p and ase1p

Budding yeast Ase1 has previously been shown to be dephosphorylated by Cdc14 at the end of mitosis (Khmelinskii et al., 2007), suggesting a role for the cyclin-dependent kinase Cdk1 and its antagonist phosphatase Cdc14 in the regulation of Ase1 during the cell cycle. To determine if the Cdk1-Cdc14 pair also regulates klp9p and ase1p in fission yeast, we examined their localization at the spindle and the effects of their activity on klp9p and ase1p. Fission yeast cdc13p (homolog of cyclin-B and binding partner of cdc2p, the homolog of Cdk1) and clp1p (homolog of Cdc14) have been shown previously to localize to the spindle at mitosis (Cueille et al., 2001; Trautmann et al., 2004; Trautmann et al., 2001; Wolfe et al., 2006). Consistent with these findings, we showed that cdc13p was associated with the spindle until the onset of anaphase B (Fig. 4A). There was no visible presence of cdc13p at the midzone during anaphase B. In contrast, clp1p appeared to concentrate at the spindle midzone during anaphase B in an antagonistic manner (Fig. 4A). This differential localization at the spindle during anaphase B suggested that cdc2p and clp1p may regulate the phosphorylation states of klp9p and ase1p. To test this hypothesis, we probed for phosphorylation and dephosphorylation of klp9p and ase1p by cdc2p and clp1p, respectively.

A previous phosphoproteomic mass-spectrometry study in fission yeast revealed specific cdc2p-dependent phosphorylation sites on klp9p (3 sites: S598, S605, S611) and ase1p (4 sites: S640, S683, S688, S693) during mitosis (Wilson-Grady et al., 2008). We created phosphoinhibit versions of klp9p and ase1p by mutating the serine into alanine (S>A) at all the reported consensus cdc2p-dependent phosphorylation motifs (Wilson-Grady et al., 2008). We note that individual mutations yielded only minor effects. We then performed *in vitro* phosphorylation assays using recombinant cdc2p, clp1p, klp9p, ase1p, $klp9p^{S>A}$, and $ase1p^{S>A}$. Where as wildtype klp9p and ase1p were highly phosphorylated by cdc2p, $klp9p^{S>A}$ and $ase1p^{S>A}$ showed a dramatic decrease in cdc2p-dependent phosphorylation (Fig. 4B). Interestingly, our blot revealed residual minor phosphorylation signals in both $klp9p^{S>A}$ and $ase1p^{S>A}$, suggesting that other cdc2p-dependent phosphorylation sites may be present. We next performed dephosphorylation assays on the phosphorylated proteins. The cdc2p-phosphorylated klp9p and ase1p products showed significant, but not complete, dephosphorylation by clp1p (Fig. 4C). We hypothesize that cdc2p phosphorylates both klp9p and ase1p prior to anaphase B. At anaphase B onset, cdc2p activity is inhibited by clp1p (Wolfe et al., 2006), and clp1p may dephosphorylate both klp9p and ase1p. One function of cdc2p-dependent phosphorylation is to allow ase1p to transit from the cytoplasm into the nucleus during the G_2/M transition (Fig. 4D and 4E). Once ase1p enters the nucleus and binds to the spindle, a second function of phosphorylation may be to prevent the physical interactions of klp9p and ase1p at the spindle midzone until anaphase B onset, when clp1p-dependent dephosphorylation of klp9p and ase1p allows the motor and MAP to physically interact for proper spindle elongation.

Klp9p and ase1p interaction requires dephosphorylation

To test this hypothesis, we performed *in vitro* binding assays with recombinant wildtype (i.e., not phosphorylated) and phosphomimic klp9p and ase1p. Phosphomimic versions of klp9p and ase1p were created by mutating the serine into aspartic acid (S>D) at all the reported consensus cdc2p-dependent phosphorylation sites (Wilson-Grady et al., 2008). With the exception of the phosphomimic klp9p$^{S>D}$ and ase1p$^{S>D}$, which exhibited little or no binding, all other combinations of klp9p and ase1p phosphorylation states exhibited strong differential bindings, with klp9p^{wt} and ase1p^{wt} exhibiting the strongest affinity based on the blot signal (Fig. 5A). We hypothesize that clp1p-dependent dephosphorylation of both klp9p and ase1p at the onset of anaphase B enables physical interactions of motor and MAP to occur at the spindle midzone.

We next examined the consequences of the failure of klp9p and ase1p to interact at anaphase B. We reasoned that klp9p and ase1p would not physically interact if they remained phosphorylated at anaphase B (Fig. 5A). One way to achieve this would be to use the phosphomimic *klp9*$^{S>D}$ and *ase1*$^{S>D}$. A second way would be to use the phosphatase inactive mutant *clp1*^{off} (Wolfe et al., 2006), which would fail to deactivate cdc2p and fail to dephosphorylate klp9p and ase1p. We analyzed klp9p and ase1p localization and spindle dynamics in the inactive mutant *clp1*^{off}, and the double phosphomimic mutant *ase1*$^{S>D}$-*klp9*$^{S>D}$. In contrast to wildtype cells (Fig. 5C), both the *clp1*^{off} and *ase1*$^{S>D}$-*klp9*$^{S>D}$ strains exhibited dispersed klp9p and ase1p localization with no clear focus at the spindle midzone throughout anaphase B (Fig. 5B and 5C), which is consistent with the hypothesis that klp9p-ase1p midzone localization requires clp1p-dependent dephosphorylation of both motor and MAP.

Further, whereas wildtype cells exhibited stereotypical anaphase B velocity (0.68 ± 0.09 n=11 μm/min), mutants *clp1*^{off} and *ase1*$^{S>D}$-*klp9*$^{S>D}$ cells showed significantly decreased spindle velocities (0.35 ± 0.05 n=9 and 0.48 ± 0.08 n=12 μm/min, respectively) (Fig. 5D). We noted that while spindle velocities of *ase1*$^{S>D}$-*klp9*$^{S>D}$ double mutant cells are expectedly less than those of wildtype cells, they are unexpectedly more than those of single mutant *klp9Δ* cells – compare 0.68 μm/min (wt), 0.29 μm/min (*klp9Δ*), and 0.48 μm/min (*ase1*$^{S>D}$-*klp9*$^{S>D}$) (compare Fig. 2D and 5D). Indeed, *ase1*$^{S>D}$-*klp9*$^{S>D}$ velocity is half-way between wildtype and the basal *klp9Δ* velocity, i.e., the presence of klp9p, even when it does not bind to ase1p, can produce intermediate sliding velocity at ~50% attenuation between wildtype maximum velocity and basal *klp9Δ* velocity (wt > *ase1*$^{S>D}$-*klp9*$^{S>D}$ > *klp9Δ*). How can klp9p binding to ase1p produce maximum velocity? We have addressed this using computer simulation (see below).

FRAP analyses suggest an *in vivo* interaction between klp9p and ase1p

To establish possible *in vivo* interaction of klp9p or ase1p, we performed FRAP experiments on cells expressing either GFP-klp9p or ase1p-GFP under the wildtype, *ase1Δ*, or *clp1*^{off} cell background (Fig. 6A and 6B). We reasoned that if klp9p and ase1p are physically interacting, they would have the same mobility, and more over, they would be less mobile as a complex than if they were separated individually. We note that due to the complexity of the experiment (e.g., the spindle is actively elongating at anaphase B, the relatively large FRAP region that covers half of the spindle midzone and thus bleaches half of the available proteins, and the processive nature of motors (Kapitein et al., 2005) and diffusive nature of MAPs (Kapitein et al., 2008a)), it may not be meaningful to extract rate contants and recovery times. We chose instead to analyze the relative percentage recovery of the different proteins. Within the 250-sec of measurement, both GFP-klp9p and ase1p-GFP showed the same low relatively recovery in wildtype cells (Fig. 6C), at 10 ± 6% n=3 and 7 ± 5% n=5,

respectively. In contrast, in the absence of either the MAP (*ase1Δ*) or the motor (*klp9Δ*), klp9p and ase1p were more mobile (Fig. 6C), with recovery of 58 ± 21% n=5 and 36 ± 16% n=4, respectively. In the *clp1*^{off} mutant, where klp9p and ase1p are expected to not interact, klp9p and ase1p were also more mobile than in wildtype (Fig. 6C), with recovery of 25 ± 8% n=3 and 61 ± 15% n=3, respectively. Finally, FRAP of the double phosphomimic mutant *ase1*$^{S>D}$-*klp9*$^{S>D}$ also showed motor and MAP to be more mobile than wildtype (Fig. S1). Taken together, we interpret these results as consistent with an *in vivo* interaction between klp9p and ase1p, and that the interaction is dependent on clp1p function.

Cytosim simulation reveals ase1p-klp9p antiparallel binding to microtubules

Tretrameric kinesin-5 Eg5 has been shown to be flexible and can twist as it cross-links and moves on two microtubules *in vitro* (Kapitein et al., 2005). Our current work shows that klp9p is a tetrameric kinesin-6 which binds microtubules independently of its phosphorylation state, but binds to ase1p in a clp1p-dependent manner. We previously reported that ase1p may be a rigid dimer with an antiparallel configuration that binds two microtubules into a rigid antiparallel bundle (Janson et al., 2007). Therefore, we hypothesized that klp9p, like Eg5, is a flexible tetramer that can adopt both parallel and antiparallel configurations, but that binding of klp9p to antiparallel ase1p locks klp9p into an antiparallel state (Fig. 7A). The parallel configuration of klp9p would not produce microtubule sliding. The antiparallel configuration of klp9p would produce maximal sliding velocity. Intermediate sliding velocities would be produced when some klp9p binds parallelly and other binds antiparallelly. We tested this hypothesis using the simulation program Cytosim (Nedelec and Foethke, 2007).

Cytosim has been used previously to model coordination between klp2p, ase1p, and microtubules in bringing about proper microtubule antiparallel organization (Janson et al., 2007). We note that the current simulation does not attempt to describe all aspects of anaphase B. It only tests the hypothesis that binding of klp9p in an antiparallel configuration would produce the maximal spindle elongation velocity. Our model assumes an initial bipolar spindle composed of five microtubules with lengths of 3-μms in each half of the spindle (Fig. 7A). The overlapping midzone was set initially at 3-μms (Fig. 7A). A notable feature of the anaphase B fission yeast spindle is the high concentration of ase1p and klp9p at the midzone (Fig. 3), and it is possible that the effects of finite microtubule binding sites could affect spindle elongation. This property is represented in our model by imposing an 8-nm site spacing, where each site can be occupied by a single motor or MAP. The motor moves in discrete steps of 8-nm and can move only if the adjacent site is unoccupied. As the kinetic parameters of klp9p are currently unknown, we set the physical properties of klp9p to be similar to Eg5 because of their shared tetrameric structure and their related roles in anaphase B (Fig. 7B) (Kapitein et al., 2008b; Kwok et al., 2006; Valentine et al., 2006a; Valentine et al., 2006b).

The first simulation involves the spindle, described above, and 120 klp9p tetramers. This is the simplest model that results in spindle elongation, and can be considered a simulation of the *ase1Δ* mutant. In this model, no ase1p molecules were present, and klp9p motility is therefore not impeded by the presence of ase1p on the microtubule lattice. Klp9p can adopt either a parallel configuration (bundling) or an antiparallel configuration (force production). This model resulted in spindles that elongate at an average rate that is similar to that observed in *ase1Δ* cells of 0.48 ± 0.15 μm/min (n=11) (Fig. 7D).

The second model is identical to the first, but with the addition of 100 dimers of the bundling protein ase1p. In this model, there are no direct interactions between ase1p and

klp9p, and klp9p is free to adopt either a parallel or antiparallel configuration, which can be considered a simulation of the *clp1*^{off} mutant. The properties of ase1p are similar to those used to model interphase microtubule bundles (Janson et al., 2007), except that the molecule acts as a bridge with a fixed distance between the bundled microtubules. There are also two stiffness components, a component that resists microtubule sliding and a second component that resists the separation of bundled microtubules. Single molecule studies have shown that the ase1p dimer diffuses freely on the microtubule lattice (Kapitein et al., 2008a), so the component resisting microtubule sliding is set to zero in this and other models involving ase1p. The reduced spindle elongation rate of 0.35 ± 0.05 μm/min (n=9) observed in the *clp1*^{off} mutant is also reproduced by this model (Fig. 7C and 7D). It is notable that the model maintains a constant spindle elongation velocity despite a decrease in the length of microtubule overlap at the midzone, as is also observed experimentally (compare Fig. 5D and 7C). The reduced spindle elongation speed, exhibited by the model, is caused by reduced klp9p binding and impeded motility caused by the presence of ase1p dimers on the microtubule lattice. Kymographs of simulated *ase1Δ* cells also showed that klp9p is less focused at the spindle midzone compared to wildtype, in agreement with experiments (compare Fig. 5C and Fig. 7E).

The final model is identical to the second, but here klp9p binds preferentially in an antiparallel configuration, which is expected to be the case in wildtype cells. We did not directly model the physical interaction between klp9p and ase1p, but instead adjusted the properties of klp9p so that it binds microtubules preferentially in an antiparallel configuration and has a slightly higher microtubule association rate. With these adjustments the model reproduced the spindle velocity of 0.68 ± 0.09 μm/min (n=11) observed in wildtype cells (Fig. 7D). Our simple models recapitulated the experimental results, and therefore showed how specific binding of klp9p to microtubules in an antiparallel orientation could increase the rate of spindle elongation, although this effect could also be explained by other mechanisms (see Discussions).

Taken together, our current work describes a novel function for the kinesin-6 klp9p in anaphase B spindle elongation, and a novel mode of klp9p and ase1p interaction which is controlled by phosphorylation (Fig. 7F).

Discussions

Our current work examined all individual motors which may be involved in anaphase B spindle elongation in fission yeast, and found that the kinesin-6 klp9p plays a major role (Fig. 1E). We suggest a mechanism whereby a cdc2p and clp1p phosphorylation switch controls the interactions of klp9p and ase1p at the spindle midzone to initiate anaphase B spindle elongation (Fig. 7F). Key to this mechanism may be the physical binding of the tetrameric kinesin-6 motor klp9p to the microtubule antiparallel-bundling MAP ase1p. Imaging and FRAP analyses supported the conclusion of an *in vivo* interaction (Fig. 6), and IP analyses confirmed an *in vitro* interaction between klp9p and ase1p (Fig. 5A). Klp9p-ase1p binding in turn biases the orientation of the motor from being naturally flexible (Kapitein et al., 2005), to the more rigid and antiparallel configuration of the MAP (Janson et al., 2007). This conformational change may increase motor efficiency in microtubule sliding, as shown by computer simulations (Fig. 7). The motor-MAP conformational change is an attractive model, and will required future single-molecule or structural analyses to confirm.

Which other motors may contribute to microtubule sliding during anaphase B? Klp9p produces ~50% of the anaphase B velocity (Fig. 1E and 2D). In the absence of klp9p, there is a residual ~0.3 μm/min spindle elongation velocity at room temperature (Fig. 1E and 2D).

Fission yeast has a second mitotic kinesin, kinesin-5 cut7p, which has been reported to localize to the spindle midzone, and whose temperature-sensitive mutation caused mono-polar spindles (Hagan and Yanagida, 1990;Hagan and Yanagida, 1992). This suggests that cut7p acts at an earlier stage of mitosis to organize the bipolar spindle. Our studies extend these previous works by looking for possible roles of cut7p at anaphase B using the *cut7-24* temperature sensitive mutant and a new temperature control device. We showed that the *cut7-24* mutant did not decrease the anaphase B spindle elongation velocity (Fig. 1C and 1E). Consistent with this finding, cut7p-3GFP does not localized to the spindle midzone during anaphase B (Fig. 1D). Lack of localization of cut7p-3GFP at the spindle midzone in this study appears different than localization of immunofluorescent-staining of cut7p to the spindle midzone in mitosis (but not the spindle midzone in meiosis) (Hagan and Yanagida, 1990;Hagan and Yanagida, 1992). One explanation may be that anti-cut7p antibodies used for immunofluorescence may cross-react with other motors. We favor the explanation that cut7p may act in a redundant and back-up manner with klp9p to ensure anaphase B spindle elongation. In deed, whereas we did not observe cut7p-3GFP at the spindle midzone in wildtype cells (Fig. 1D), our preliminary result shows that cut7p-3GFP does localize to the spindle midzone in *klp9Δ* mutant cells, suggesting possible redundant roles (our unpublished data). In budding yeast, both kinesins and dynein play cooperative roles in bringing about proper anaphase spindle elongation (Saunders et al., 1995). Our current study deals with individual motors, and showed that dynein deletion alone has no effect on spindle elongation (Fig. 1E). Future studies will explore combinatorial relationships among the different motors for a fuller understanding of anaphase B.

Anaphase B is a prominent phase of mitosis, marked by an increase in spindle length, up to 1.5 – 4-times of the initial metaphase/anaphase A spindle length in different organisms (Hayashi et al., 2007). To date, physical mechanisms producing anaphase B have primarily focused on the kinesin-5 motors (Scholey et al., 2003; Sharp et al., 2000). Kinesin-6 motors have been assigned regulatory roles at the end of mitosis at the transition to cytokinesis (Gruneberg et al., 2006; Kuriyama et al., 2002; Matuliene and Kuriyama, 2002; Mishima et al., 2002). In deed, the centralspindlin complex, which contains kinesin-6, is regulated by aurora B kinase for proper cytokinesis (Mishima and Glotzer, 2003; Mishima et al., 2002; Mishima et al., 2004). The involvement of fission yeast klp9p in anaphase B spindle elongation suggests a novel function for the kinesin-6 family of motors. Our simulations, while not meant to represent actual klp9p kinetics, were useful in predicting and recapitulating our experimental results by showing trends in elongation velocities and how these rates can be altered by specific configurations of klp9p (Fig. 7). Other models are also plausible. For example, klp9p-ase1p interaction can serve to concentrate klp9p at the spindle midzone, and that cooperative effects of motors can lead to more efficient velocity. Future studies will need to examine the evolution of the multiple functions associated with the kinesin-6 family of mitotic motors.

The MAP Ase1/PRC1 appears to be a major scaffolding protein at the spindle midzone. The fission yeast ase1p is a substrate for cdc2p and clp1p phosphoregulation, which allows for binding to klp9p (this study). The budding yeast Ase1 and human PRC1 may also be a substrate for Cdk1 and Cdc14, and other regulatory proteins such as the Ipl1/arora-B kinase (Jiang et al., 1998; Khmelinskii et al., 2007; Kotwaliwale et al., 2007). Our studies add to the emerging concept that the spindle midzone, with motors and MAPs and kinases and phosphatases, is a crowded mechanical and chemical machine (Glotzer, 2005).

Experimental Procedures

Experimental procedures are described in the Supplemental.

Supplementary Material

Refer to Web version on PubMed Central for supplementary material.

Acknowledgments

We thank Anabelle Decottignies, Fred Chang, Kathy Gould, Ian Hagan, Dan McCollum, and Paul Nurse for yeast strains and reagents. We thank Andrea Stout for expert technical FRAP assistance. We also thank members of Erfei Bi Lab and members of the MBL Physiology 2007 for helpful discussions and advice. F.J.N is supported by BioMS, J.W. is supported by the Volkswagen-Stiftung. G.V-C. is supported by ARC. The Tran Lab is supported by grants from NIH, ACS, HFSP, and ANR, FRM, and LaLigue. C.F., I.L., G. V-C., and P.T.T created the reagents, performed the experiments, and analyzed the data. J.W. and F.N. performed the computer simulations. C.F., J.W., F.N. and P.T.T. wrote the paper and all authors made comments.

References

Bahler J, Wu JQ, Longtine MS, Shah NG, McKenzie A 3rd, Steever AB, Wach A, Philippsen P, Pringle JR. Heterologous modules for efficient and versatile PCR-based gene targeting in Schizosaccharomyces pombe. Yeast 1998;14:943–951. [PubMed: 9717240]

Brazer SC, Williams HP, Chappell TG, Cande WZ. A fission yeast kinesin affects Golgi membrane recycling. Yeast 2000;16:149–166. [PubMed: 10641037]

Browning H, Hayles J, Mata J, Aveline L, Nurse P, McIntosh JR. Tea2p is a kinesin-like protein required to generate polarized growth in fission yeast. J Cell Biol 2000;151:15–28. [PubMed: 11018050]

Carminati JL, Stearns T. Microtubules orient the mitotic spindle in yeast through dynein-dependent interactions with the cell cortex. J Cell Biol 1997;138:629–641. [PubMed: 9245791]

Cheeseman IM, Desai A. Molecular architecture of the kinetochore-microtubule interface. Nat Rev Mol Cell Biol 2008;9:33–46. [PubMed: 18097444]

Cueille N, Salimova E, Esteban V, Blanco M, Moreno S, Bueno A, Simanis V. Flp1, a fission yeast orthologue of the s. cerevisiae CDC14 gene, is not required for cyclin degradation or rum1p stabilisation at the end of mitosis. J Cell Sci 2001;114:2649–2664. [PubMed: 11683392]

Fink G, Schuchardt I, Colombelli J, Stelzer E, Steinberg G. Dynein-mediated pulling forces drive rapid mitotic spindle elongation in Ustilago maydis. Embo J 2006;25:4897–4908. [PubMed: 17024185]

Garcia MA, Koonrugsa N, Toda T. Spindle-kinetochore attachment requires the combined action of Kin I-like Klp5/6 and Alp14/Dis1-MAPs in fission yeast. Embo J 2002a;21:6015–6024. [PubMed: 12426374]

Garcia MA, Koonrugsa N, Toda T. Two kinesin-like Kin I family proteins in fission yeast regulate the establishment of metaphase and the onset of anaphase A. Curr Biol 2002b;12:610–621. [PubMed: 11967147]

Glotzer M. The molecular requirements for cytokinesis. Science 2005;307:1735–1739. [PubMed: 15774750]

Gruneberg U, Neef R, Li X, Chan EH, Chalamalasetty RB, Nigg EA, Barr FA. KIF14 and citron kinase act together to promote efficient cytokinesis. J Cell Biol 2006;172:363–372. [PubMed: 16431929]

Guse A, Mishima M, Glotzer M. Phosphorylation of ZEN-4/MKLP1 by aurora B regulates completion of cytokinesis. Curr Biol 2005;15:778–786. [PubMed: 15854913]

Hagan I, Yanagida M. Novel potential mitotic motor protein encoded by the fission yeast cut7+ gene. Nature 1990;347:563–566. [PubMed: 2145514]

Hagan I, Yanagida M. Kinesin-related cut7 protein associates with mitotic and meiotic spindles in fission yeast. Nature 1992;356:74–76. [PubMed: 1538784]

Hagan IM. The fission yeast microtubule cytoskeleton. J Cell Sci 1998;111(Pt 12):1603–1612. [PubMed: 9601091]

Hayashi T, Sano T, Kutsuna N, Kumagai-Sano F, Hasezawa S. Contribution of anaphase B to chromosome separation in higher plant cells estimated by image processing. Plant Cell Physiol 2007;48:1509–1513. [PubMed: 17855443]

Hiraoka Y, Ding DQ, Yamamoto A, Tsutsumi C, Chikashige Y. Characterization of fission yeast meiotic mutants based on live observation of meiotic prophase nuclear movement. Chromosoma 2000;109:103–109. [PubMed: 10855500]

Hoyt MA, He L, Loo KK, Saunders WS. Two Saccharomyces cerevisiae kinesin-related gene products required for mitotic spindle assembly. J Cell Biol 1992;118:109–120. [PubMed: 1618897]

Janson ME, Loughlin R, Loiodice I, Fu C, Brunner D, Nedelec FJ, Tran PT. Crosslinkers and motors organize dynamic microtubules to form stable bipolar arrays in fission yeast. Cell 2007;128:357–368. [PubMed: 17254972]

Jiang W, Jimenez G, Wells NJ, Hope TJ, Wahl GM, Hunter T, Fukunaga R. PRC1: a human mitotic spindle-associated CDK substrate protein required for cytokinesis. Mol Cell 1998;2:877–885. [PubMed: 9885575]

Kapitein LC, Janson ME, van den Wildenberg SM, Hoogenraad CC, Schmidt CF, Peterman EJ. Microtubule-driven multimerization recruits ase1p onto overlapping microtubules. Curr Biol 2008a;18:1713–1717. [PubMed: 18976915]

Kapitein LC, Kwok BH, Weinger JS, Schmidt CF, Kapoor TM, Peterman EJ. Microtubule cross-linking triggers the directional motility of kinesin-5. J Cell Biol 2008b;182:421–428. [PubMed: 18678707]

Kapitein LC, Peterman EJ, Kwok BH, Kim JH, Kapoor TM, Schmidt CF. The bipolar mitotic kinesin Eg5 moves on both microtubules that it crosslinks. Nature 2005;435:114–118. [PubMed: 15875026]

Kapoor TM, Mayer TU, Coughlin ML, Mitchison TJ. Probing spindle assembly mechanisms with monastrol, a small molecule inhibitor of the mitotic kinesin, Eg5. J Cell Biol 2000;150:975–988. [PubMed: 10973989]

Khmelinskii A, Lawrence C, Roostalu J, Schiebel E. Cdc14-regulated midzone assembly controls anaphase B. J Cell Biol 2007;177:981–993. [PubMed: 17562791]

Khodjakov A, La Terra S, Chang F. Laser microsurgery in fission yeast; role of the mitotic spindle midzone in anaphase B. Curr Biol 2004;14:1330–1340. [PubMed: 15296749]

Kotwaliwale CV, Frei SB, Stern BM, Biggins S. A pathway containing the Ipl1/aurora protein kinase and the spindle midzone protein Ase1 regulates yeast spindle assembly. Dev Cell 2007;13:433–445. [PubMed: 17765685]

Kurasawa Y, Earnshaw WC, Mochizuki Y, Dohmae N, Todokoro K. Essential roles of KIF4 and its binding partner PRC1 in organized central spindle midzone formation. Embo J 2004;23:3237–3248. [PubMed: 15297875]

Kuriyama R, Gustus C, Terada Y, Uetake Y, Matuliene J. CHO1, a mammalian kinesin-like protein, interacts with F-actin and is involved in the terminal phase of cytokinesis. J Cell Biol 2002;156:783–790. [PubMed: 11877456]

Kwok BH, Kapitein LC, Kim JH, Peterman EJ, Schmidt CF, Kapoor TM. Allosteric inhibition of kinesin-5 modulates its processive directional motility. Nat Chem Biol 2006;2:480–485. [PubMed: 16892050]

Loiodice I, Staub J, Setty TG, Nguyen NP, Paoletti A, Tran PT. Ase1p organizes antiparallel microtubule arrays during interphase and mitosis in fission yeast. Mol Biol Cell 2005;16:1756–1768. [PubMed: 15689489]

Maiato H, Sampaio P, Sunkel CE. Microtubule-associated proteins and their essential roles during mitosis. Int Rev Cytol 2004;241:53–153. [PubMed: 15548419]

Mallavarapu A, Sawin K, Mitchison T. A switch in microtubule dynamics at the onset of anaphase B in the mitotic spindle of Schizosaccharomyces pombe. Curr Biol 1999;9:1423–1426. [PubMed: 10607565]

Matuliene J, Kuriyama R. Kinesin-like protein CHO1 is required for the formation of midbody matrix and the completion of cytokinesis in mammalian cells. Mol Biol Cell 2002;13:1832–1845. [PubMed: 12058052]

Mishima M, Glotzer M. Cytokinesis: a logical GAP. Curr Biol 2003;13:R589–591. [PubMed: 12906808]

Mishima M, Kaitna S, Glotzer M. Central spindle assembly and cytokinesis require a kinesin-like protein/RhoGAP complex with microtubule bundling activity. Dev Cell 2002;2:41–54. [PubMed: 11782313]

Mishima M, Pavicic V, Gruneberg U, Nigg EA, Glotzer M. Cell cycle regulation of central spindle assembly. Nature 2004;430:908–913. [PubMed: 15282614]

Mogilner A, Wollman R, Civelekoglu-Scholey G, Scholey J. Modeling mitosis. Trends Cell Biol 2006;16:88–96. [PubMed: 16406522]

Mollinari C, Kleman JP, Jiang W, Schoehn G, Hunter T, Margolis RL. PRC1 is a microtubule binding and bundling protein essential to maintain the mitotic spindle midzone. J Cell Biol 2002;157:1175–1186. [PubMed: 12082078]

Nabeshima K, Nakagawa T, Straight AF, Murray A, Chikashige Y, Yamashita YM, Hiraoka Y, Yanagida M. Dynamics of centromeres during metaphase-anaphase transition in fission yeast: Dis1 is implicated in force balance in metaphase bipolar spindle. Mol Biol Cell 1998;9:3211–3225. [PubMed: 9802907]

Nedelec FJ, Foethke D. Collective Langevin dynamics of flexible cytoskeletal fibers. New Journal of Physics 2007;9:427.

Nguyen-Ngoc T, Afshar K, Gonczy P. Coupling of cortical dynein and G alpha proteins mediates spindle positioning in Caenorhabditis elegans. Nat Cell Biol 2007;9:1294–1302. [PubMed: 17922003]

O'Connell CB, Wang YL. Mammalian spindle orientation and position respond to changes in cell shape in a dynein-dependent fashion. Mol Biol Cell 2000;11:1765–1774. [PubMed: 10793150]

Pidoux AL, LeDizet M, Cande WZ. Fission yeast pkl1 is a kinesin-related protein involved in mitotic spindle function. Mol Biol Cell 1996;7:1639–1655. [PubMed: 8898367]

Roof DM, Meluh PB, Rose MD. Kinesin-related proteins required for assembly of the mitotic spindle. J Cell Biol 1992;118:95–108. [PubMed: 1618910]

Sagolla MJ, Uzawa S, Cande WZ. Individual microtubule dynamics contribute to the function of mitotic and cytoplasmic arrays in fission yeast. J Cell Sci 2003;116:4891–4903. [PubMed: 14625383]

Saunders WS, Koshland D, Eshel D, Gibbons IR, Hoyt MA. Saccharomyces cerevisiae kinesin- and dynein-related proteins required for anaphase chromosome segregation. J Cell Biol 1995;128:617–624. [PubMed: 7860634]

Schmidt DJ, Rose DJ, Saxton WM, Strome S. Functional analysis of cytoplasmic dynein heavy chain in Caenorhabditis elegans with fast-acting temperature-sensitive mutations. Mol Biol Cell 2005;16:1200–1212. [PubMed: 15616192]

Scholey JM, Brust-Mascher I, Mogilner A. Cell division. Nature 2003;422:746–752. [PubMed: 12700768]

Schuyler SC, Liu JY, Pellman D. The molecular function of Ase1p: evidence for a MAP-dependent midzone-specific spindle matrix. Microtubule-associated proteins. J Cell Biol 2003;160:517–528. [PubMed: 12591913]

Sharp DJ, Rogers GC, Scholey JM. Microtubule motors in mitosis. Nature 2000;407:41–47. [PubMed: 10993066]

Straight AF, Sedat JW, Murray AW. Time-lapse microscopy reveals unique roles for kinesins during anaphase in budding yeast. J Cell Biol 1998;143:687–694. [PubMed: 9813090]

Tanaka TU, Desai A. Kinetochore-microtubule interactions: the means to the end. Curr Opin Cell Biol 2008;20:53–63. [PubMed: 18182282]

Terenna CR, Makushok T, Velve-Casquillas G, Baigl D, Chen Y, Bornens M, Paoletti A, Piel M, Tran PT. Physical mechanisms redirecting cell polarity and cell shape in fission yeast. Curr Biol 2008;18:1748–1753. [PubMed: 19026544]

Tolic-Norrelykke IM, Sacconi L, Thon G, Pavone FS. Positioning and elongation of the fission yeast spindle by microtubule-based pushing. Curr Biol 2004;14:1181–1186. [PubMed: 15242615]

Tran PT, Paoletti A, Chang F. Imaging green fluorescent protein fusions in living fission yeast cells. Methods 2004;33:220–225. [PubMed: 15157889]

Trautmann S, Rajagopalan S, McCollum D. The S. pombe Cdc14-like phosphatase Clp1p regulates chromosome biorientation and interacts with Aurora kinase. Dev Cell 2004;7:755–762. [PubMed: 15525536]

Trautmann S, Wolfe BA, Jorgensen P, Tyers M, Gould KL, McCollum D. Fission yeast Clp1p phosphatase regulates G2/M transition and coordination of cytokinesis with cell cycle progression. Curr Biol 2001;11:931–940. [PubMed: 11448769]

Troxell CL, Sweezy MA, West RR, Reed KD, Carson BD, Pidoux AL, Cande WZ, McIntosh JR. pkl1(+)and klp2(+): Two kinesins of the Kar3 subfamily in fission yeast perform different functions in both mitosis and meiosis. Mol Biol Cell 2001;12:3476–3488. [PubMed: 11694582]

Valentine MT, Fordyce PM, Block SM. Eg5 steps it up! Cell Div 2006a;1:31. [PubMed: 17173688]

Valentine MT, Fordyce PM, Krzysiak TC, Gilbert SP, Block SM. Individual dimers of the mitotic kinesin motor Eg5 step processively and support substantial loads in vitro. Nat Cell Biol 2006b; 8:470–476. [PubMed: 16604065]

Verni F, Somma MP, Gunsalus KC, Bonaccorsi S, Belloni G, Goldberg ML, Gatti M. Feo, the Drosophila homolog of PRC1, is required for central-spindle formation and cytokinesis. Curr Biol 2004;14:1569–1575. [PubMed: 15341744]

West RR, Malmstrom T, McIntosh JR. Kinesins klp5(+) and klp6(+) are required for normal chromosome movement in mitosis. J Cell Sci 2002;115:931–940. [PubMed: 11870212]

West RR, Malmstrom T, Troxell CL, McIntosh JR. Two related kinesins, klp5+ and klp6+, foster microtubule disassembly and are required for meiosis in fission yeast. Mol Biol Cell 2001;12:3919–3932. [PubMed: 11739790]

Wilson-Grady JT, Villen J, Gygi SP. Phosphoproteome analysis of fission yeast. J Proteome Res 2008;7:1088–1097. [PubMed: 18257517]

Wolfe BA, McDonald WH, Yates JR 3rd, Gould KL. Phospho-regulation of the Cdc14/Clp1 phosphatase delays late mitotic events in S. pombe. Dev Cell 2006;11:423–430. [PubMed: 16950131]

Yamashita A, Sato M, Fujita A, Yamamoto M, Toda T. The roles of fission yeast ase1 in mitotic cell division, meiotic nuclear oscillation, and cytokinesis checkpoint signaling. Mol Biol Cell 2005;16:1378–1395. [PubMed: 15647375]

Zhu C, Bossy-Wetzel E, Jiang W. Recruitment of MKLP1 to the spindle midzone/midbody by INCENP is essential for midbody formation and completion of cytokinesis in human cells. Biochem J 2005;389:373–381. [PubMed: 15796717]

Zhu C, Jiang W. Cell cycle-dependent translocation of PRC1 on the spindle by Kif4 is essential for midzone formation and cytokinesis. Proc Natl Acad Sci U S A 2005;102:343–348. [PubMed: 15625105]

Zhu C, Lau E, Schwarzenbacher R, Bossy-Wetzel E, Jiang W. Spatiotemporal control of spindle midzone formation by PRC1 in human cells. Proc Natl Acad Sci U S A 2006;103:6196–6201. [PubMed: 16603632]

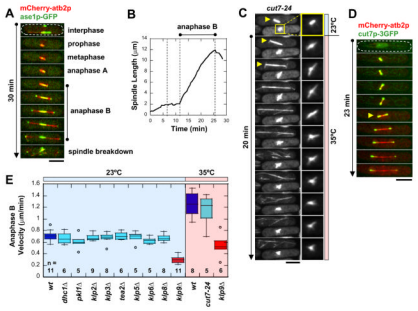

Figure 1. Novel fission yeast kinesin-6 klp9p is involved in anaphase B spindle elongation

(A) Time-lapsed images of cell expressing mCherry-atb2p (tubulin) and ase1p-GFP through different phases of mitosis. Ase1p stabilizes the spindle midzone throughout anaphase B (Loiodice et al., 2005; Yamashita et al., 2005). Bar, 5 μm.

(B) Typical wildtype spindle length vs. time plot. Anaphase B is marked by a dramatic increase in spindle length and spindle elongation velocity.

(C) Temperature shift experiment of *cut7-24* mutant cells expressing GFP-atb2p. Within two minutes of shifting to the restrictive temperature of 35°C, the metaphase cell (bottom cell) immediately exhibited spindle collapse, which became a mono-polar spindle (see enlargement box) (Hagan and Yanagida, 1990; Hagan and Yanagida, 1992). In contrast, the anaphase cell (top cell) continued through anaphase B spindle elongation (yellow arrow). Bar, 5 μm.

(D) Time-lapsed images of cell expressing mCherry-atb2p (tubulin) and cut7p-3GFP. No cut7p-3GFP was observed at the anaphase B spindle midzone. Bar, 5 μm.

(E) Box plot comparison of anaphase B spindle elongation velocities in wildtype cells and motor mutant cells. Only *klp9Δ* shows a significant decrease in velocity. At the higher temperature required for *cut7-24*, spindle elongation velocity increased for both wildtype and *klp9Δ* correspondingly.

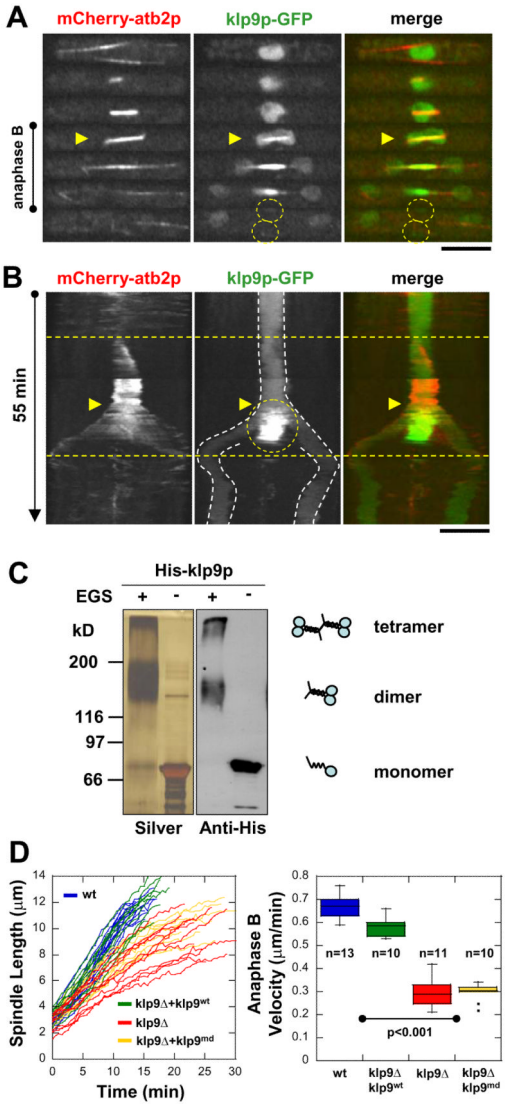

Figure 2. Klp9p may be a tetramer that slides the bipolar spindle apart during anaphase B

(A) Time-lapsed images of cell expressing mCherry-atb2 (tubulin) and klp9p-GFP. During interphase, prophase, metaphase and anaphase A, klp9p-GFP is located in the nucleoplasm. At the onset of anaphase B (yellow arrow heads), klp9p-GFP goes to the spindle and the spindle midzone. At the end of anaphase B, the spindle breaks down, and klp9p-GFP is transiently at the site of the presumptive contractile ring (yellow dashed circles).

(B) Kymographs of klp9p dynamics throughout the cell cycle. Mitosis in fission yeast lasts ~30 min. Anaphase B (yellow arrow heads) marks a relatively fast spindle elongation rate of ~0.7 μm/min and lasts ~12 min before spindle breakdown. Klp9p-GFP localizes to the spindle at anaphase B onset, and focuses to the spindle midzone throughout anaphase B (yellow dashed circle). Dashed white lines mark the position of the nucleus and divided nuclei. Bar, 5 μm.

(C) EGS cross-linking of recombinant His-klp9p revealed dimers and tetramers.

(D) Comparative plot of spindle length vs. time and box plot of anaphase B spindle elongation velocities of wildtype cells (wt, blue), *klp9Δ* cells expressing exogenous wildtype *klp9* (*klp9Δ+klp9*^{wt}, green), *klp9Δ* cells (*klp9Δ*, red), and *klp9Δ* cells expressing exogenous *klp9* motor dead mutant (*klp9*^{md}, yellow).

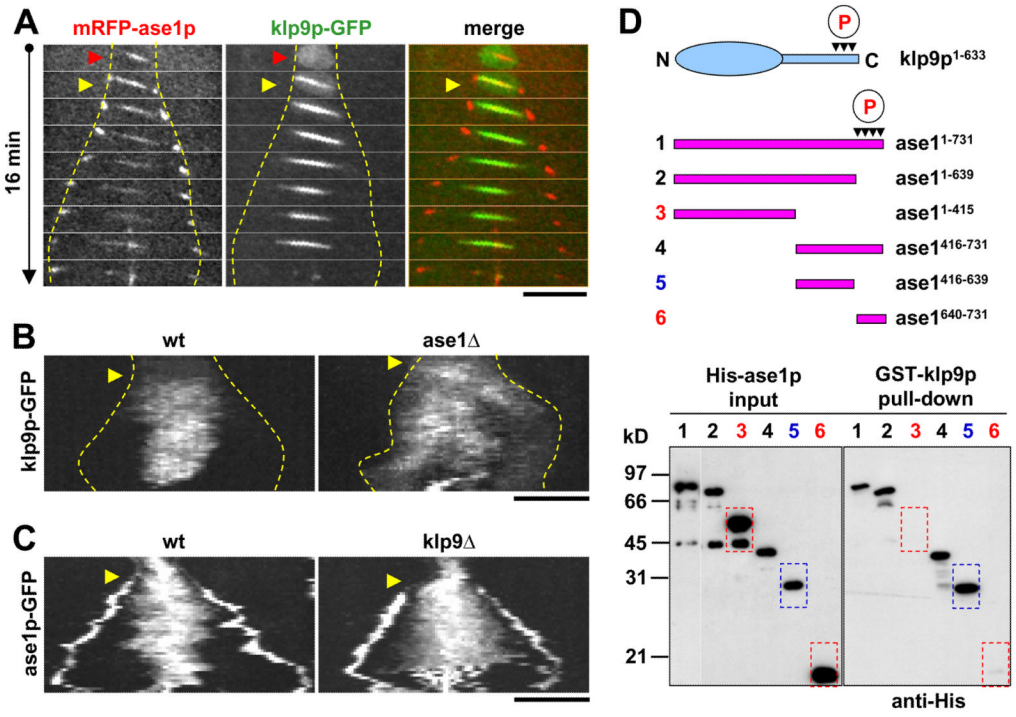

Figure 3. Klp9p interacts with the microtubule bundler ase1p *in vivo* and *in vitro*, and requires ase1p to focus at the spindle midzone

(A) *In vivo* colocalization of klp9p and ase1p at the spindle midzone during anaphase B. Time-lapsed images of cell expressing mRFP-ase1p and klp9p-GFP. Dashed yellow lines show positions of the spindle poles. The microtubule antiparallel bundler mRFP-ase1p localizes early on to the spindle (red arrow head). Subsequently, at the onset of anaphase B (yellow arrow heads), klp9p-GFP colocalizes with mRFP-ase1p at the spindle and spindle midzone. Bar, 5 μm.

(B) Kymographs of wildtype and *ase1Δ* cells expressing klp9p-GFP. (Anaphase B onset, yellow arrows). The wildtype cell shows a clear focusing of klp9p-GFP at the spindle midzone as anaphase B progressed. In contrast, the *ase1Δ* cell fails to focus klp9p-GFP at the midzone region.

(C) Kymographs of wildtype and *klp9Δ* cells expressing ase1p-GFP. (Anaphase B onset, yellow arrows). The wildtype cell shows a clear focusing of ase1p-GFP at the spindle midzone as anaphase B progressed. In contrast, the *klp9Δ* cell fails to focus ase1p-GFP at the midzone region. Bar, 5 μm.

(D) Klp9p binds to ase1p *in vitro*. Pull-down assays of full-length recombinant GST-klp9p with different truncated versions of recombinant His-ase1p. Schematics of klp9p and ase1p, showing multiple cyclin-dependent kinase phosphorylation sites at their carboxyl termini (red circled P). Dashed red boxes (lanes 3 and 6) indicate no physical interaction. Dashed blue boxes (lane 5) indicate physical interaction.

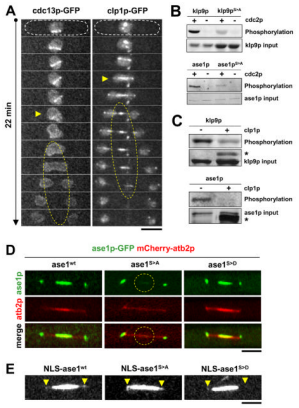

Figure 4. Kinase cdc2p (Cdk1) and its antagonist phosphatase clp1p (Cdc14) regulate the phosphorylation states of klp9p and ase1p

(A) Time-lapsed images of cells expressing either cdc13p-GFP (cyclin B, binding partner of cdc2p) or clp1p-GFP during mitosis. Prior to anaphase B, cdc13p-GFP localizes to the spindle. At anaphase B onset (yellow arrow head), cdc13p-GFP delocalizes from the spindle (yellow dashed oval). In contrast, prior to anaphase B, clp1p-GFP localizes to the spindle poles and nucleolus. At anaphase B onset (yellow arrow head), clp1p-GFP localizes to the spindle and subsequently the spindle midzone (yellow dashed oval). Bar, 5 μm.

(B) Klp9p and ase1p are phosphorylated by cdc2p *in vitro*. Recombinant His-klp9p and His-klp9p^{phosphoinhibit} (His-klp9p$^{S>A}$) and His-ase1p and His-ase1p^{phosphoinhibit} (His-ase1p$^{S>A}$) were incubated with cdc2p.

(C) Klp9p and ase1p are dephosphorylated by clp1p *in vitro*. Recombinant GST-klp9p and GST-ase1p was first phosphorylated by cdc2p. The products were next incubated with recombinant MBP-clp1p. (Asterisk * corresponds to MBP-clp1p)

(D) Ase1-phosphoinhibit version ase1p$^{S>A}$ cannot enter the nucleus during closed mitosis. Shown are cells expressing mCherry-atb2 (tubulin) and GFP-tagged ase1^{wt}, ase1^{phosphoinhibit} (ase1$^{S>A}$), or ase1^{phosphomimic} (ase1$^{S>D}$). At mitosis ase1^{wt} and ase1$^{S>D}$ localize to the spindle midzone. In contrast, ase1$^{S>A}$ is not strongly visible at the spindle midzone (yellow dashed circle). Bar, 5 μm.

(E) Dual GFP- and NLS-tagged versions of ase1^{wt}, ase1^{phosphoinhibit} (ase1$^{S>A}$), or ase1^{phosphomimic} (ase1$^{S>D}$). Prominent is the strong signal of ase1^{phosphomimic} (ase1$^{S>D}$), which now can enter the nucleus. Arrow heads mark the spindle poles. Bar, 5 μm.

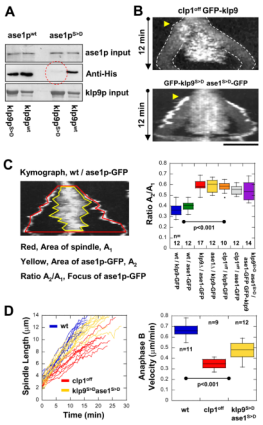

Figure 5. Dephosphorylation of klp9p and ase1p by the phosphatase clp1p (Cdc14) are required for their efficient binding and proper anaphase B spindle elongation

(A) Pull-down assays of recombinant GST-klp9p and GST-klp9p^{phosphomimic} (GST-klp9p$^{S>D}$) with recombinant His-ase1p and His-ase1p^{phosphomimic} (His-ase1p$^{S>D}$). The strongest binding is observed with GST-klp9p and His-ase1p. Bindings are also observed with either GST-klp9p or His-ase1p phosphomimic versions. No binding is observed between GST-klp9p$^{S>D}$ and His-ase1p$^{S>D}$ (red dashed circle).

(B) Kymographs of mutant *clp1*^{off} cells and double mutant *klp9*^{phosphomimic}*ase1*^{phosphomimic} (*klp9*$^{S>D}$*ase1*$^{S>D}$) cells expressing klp9p-GFP during mitosis. Mutant *clp1*^{off} cells, which have no phosphastase activity, and double mutant *klp9*$^{S>D}$*ase1*$^{S>D}$ cells show GFP-klp9p and ase1p-GFP dispersed to wider regions of the spindle. Bar, 5 μm.

(C) Quantification of klp9p and ase1p focusing at the spindle midzone. Kymograph of anaphase B shows two regions of interest: the area A_1 covered by the spindle (red boundary), and the area A_2 covered by klp9p-GFP or ase1p-GFP at the midzone (yellow boundary). We defined the ratio of the A_2/A_1 as the index of focusing. Box plot shows that klp9p-GFP and ase1p-GFP are highly focused at the spindle midzone in wildtype cells. In contrast, phospho-mutants of *klp9* and *ase1* and *clp1*^{off} show klp9p-GFP and ase1p-GFP spread out on the spindle.

(D) Comparative plot of spindle length vs. time and box plot of anaphase B spindle elongation velocity of wildtype cells (wt, blue), mutant *clp1*^{off} cells (*clp1*^{off}, red), and double mutant *klp9* ^{phosphomimic}*ase1*^{phosphomimic} cells (*klp9*$^{S>D}$*ase1*$^{S>D}$, yellow).

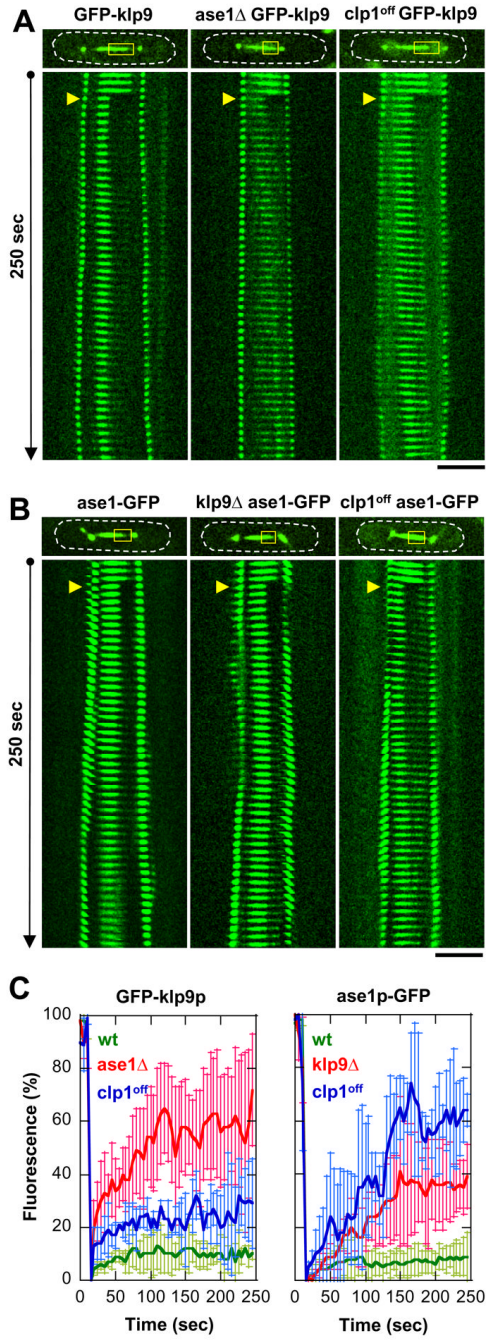

Figure 6. FRAP analysis suggests an *in vivo* interaction between klp9p and ase1p

(A) Coarse kymograph of fluorescence recovery of cells expressing GFP-klp9p under the wildtype, *ase1Δ*, or *clp1*^{off} cell background. Note that cells also express alp4p-GFP spindle pole marker to show precise spindle length and the timing of anaphase B. Yellow boxes, bleached region. Yellow arrows, FRAP start. Bar, 5 μm.

(B) Coarse kymograph of fluorescence recovery of cells expressing ase1p-GFP under the wildtype, *klp9Δ*, or *clp1*^{off} cell background.

(C) Comparative plots of fluorescence recovery after bleaching. Shown are normalized fluorescent signals with pre-bleached at 100% (mean ± sd). Left panel, GFP-klp9p in wildtype (green), *ase1Δ* (red), and *clp1*^{off} (blue). Right panel, ase1p-GFP in wildtype

(green), *ase1Δ* (red), and *clp1*^{off} (blue). Note the relatively higher mobility of klp9p and ase1p in the mutant backgrounds compared to wildtype.

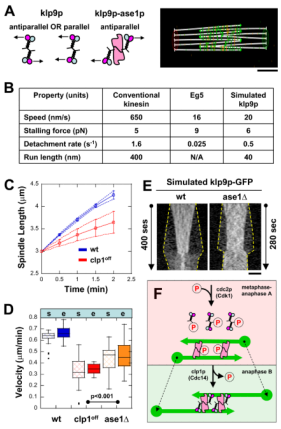

Property (units)	Conventional kinesin	Eg5	Simulated klp9p
Speed (nm/s)	650	16	20
Stalling force (pN)	5	9	6
Detachment rate (s^{-1})	1.6	0.025	0.5
Run length (nm)	400	N/A	40

Figure 7. Cytosim model of how klp9p (motor) and ase1p (MAP) interact for proper anaphase B

(A) Cytosim model assumption: klp9p is either parallel or antiparallel by itself, but is antiparallel when bound to ase1p. Bar, 1 μm.

(B) Parameters used in simulations (see text). Parameters of klp9p are assumed to be similar to Eg5, a similar mitotic kinesin.

(C) Comparative plot of spindle length vs. time and box plot of anaphase B spindle elongation velocity of simulated wildtype cells (wt, blue) and mutant *clp1^{off}* cells (*clp1^{off}*, red). Simulation reproduces the experimental results (compare with Fig. 4C).

(D) Comparative box plot of simulated (**s**) and experimental (**e**) spindle velocities for wildtype cells (wt, blue), *clp1^{off}* cells (*clp1^{off}*, red), and *ase1Δ* cells (*ase1Δ*, orange). Spindle velocities of *ase1Δ* cells are intermediate between wt and *clp1^{off}*.

(E) Comparative kymographs of simulated klp9p-GFP focusing at the middle of the spindle in wildtype and *ase1Δ* cells. Dashed yellow lines show positions of the spindle poles. In the absence of ase1p, klp9p is less focused at the spindle midzone, similar to experimental findings (compare with Fig. 3B and 5C). Bar, 1 μm.

(F) Model of how kinase cdc2p (Cdk1) and phosphatase clp1p (Cdc14) regulate the function of klp9p (motor) and ase1p (MAP) for proper anaphase B.